Applied Surface Science 608 (2023) 155099

Contents lists available at ScienceDirect

Applied Surface Science

journal homepage: www.elsevier.com/locate/apsusc

Full Length Article

Origin of interfacial charges of Al_2O_3/Si and Al_2O_3/GaN heterogeneous heterostructures

Chuanju Wang, Feras AlQatari, Vishal Khandelwal, Rongyu Lin, Xiaohang Li *

Advanced Semiconductor Laboratory, Electrical and Computer Engineering Programs, CEMSE Division, King Abdullah University of Science and Technology (KAUST), Thuwal 23955, Saudi Arabia

A B S T R A C T

Al_2O_3 is a broadly employed dielectric and significant interfacial charges occur at Al_2O_3/semiconductor interfaces. However, the charge origin is often unclear that severely impacts device engineering and design. Al_2O_3/Si and Al_2O_3/GaN are two of the most common heterogeneous heterostructures (H2s) for many crucial devices including GaN transistors and Si solar cells. While negative charges are extensively observed in Al_2O_3/Si, positive charges exist in Al_2O_3/GaN, both of which are not well understood. In this study, we performed in-depth interfacial studies of the Al_2O_3/Si and Al_2O_3/GaN H2s to clarify the origin of the interfacial charges. Stoichiometry deviations were found at the interfaces of the two H2s where Al surpasses O for Al_2O_3/GaN, whereas O dominates at the Al_2O_3/Si interface. Therefore, we propose that the different interfacial charges are caused by nonstoichiometry atomic ratios of Al_2O_3 at the interface. The study indicates the important role of the semiconductor surface on the device performance, provide a deep understanding on the origin of interfacial charges at the insulator-semiconductor interfaces.

1. Introduction

Al_2O_3 thin films with high dielectric constant (8–10) and large bandgap energy (7–9 eV) have attracted extensive interest due to vast crucial device applications [1–6]. In the semiconductor technology, Si has been the dominant substrate material in the past few decades [1–8]. In recent years, wide band gap semiconductors such as GaN and SiC have attracted much attention due to their potential application in high power and high frequency devices [9–14]. Al_2O_3 is typically employed as the surface passivation layer in Si solar cells due to numerous negative charges that occur at the interface of the Al_2O_3/Si heterogeneous heterostructure (H2) [2–6]. These negative charges can shield the minority carriers i.e. electrons from the surface of the Si solar cells, reducing the surface recombination rate [7,8]. Meanwhile, Al_2O_3 has also been widely adopted in GaN high-electron-mobility transistors (HEMTs) as the gate dielectric that suppresses the gate leakage current and enlarges the gate voltage swing [9–11]. Enhancement model GaN HEMTs can be obtained by extending the gate dielectric thickness if the charges at the interface of Al_2O_3/GaN H2 are also negative [11]. However, the positive charges occur at the interface of Al_2O_3/GaN H2 can shift the threshold voltage to a negative value, hindering the realization of enhancement model GaN HEMTs [12–14].

In the research areas of GaN HEMTs, impurities in Al_2O_3 can account for the positive charges of Al_2O_3/GaN H2. The incomplete oxidation of trimethylamine (TMA) molecules during the atomic layer deposition (ALD) process will lead to residual carbon impurities in Al_2O_3, which is in responsible for the positive charges [15,16]. In addition, Al interstitials and O vacancies inside Al_2O_3 are also considered as one source of the positive charges [17,18]. Furthermore, the positive charges occur the interface of the Al_2O_3/GaN H2 irrespective of the GaN polarity (Ga-polar and N-polar) [19].

The origin of the negative charges in Al_2O_3/Si H2 has also been discussed extensively after the laboratory and industrial implementation of Al_2O_3 as the passivation layer in Si solar cells [1–3,17,18,20–22]. In general, structural impurities inside Al_2O_3, such as O interstitials, O dangling bonds, Al vacancies, and H interstitials, are responsible for the negative charges [17,18]. Density functional theory (DFT) revealed O interstitials are in the −2 state and Al vacancies are in the −3 state in Al_2O_3; these defect levels are below the midgap of the Al_2O_3 bandgap, thereby forming stable negatively charged states [20,21]. Other proposed mechanisms attributed negative charges to the bonding configurations of Al at the interface where tetrahedrally coordinated Al remarkably surpassed the octahedrally coordinated Al at the Al_2O_3/Si interface [22,23]. The occurrence of such negative charges at the interface is independent of the orientation, doping type, and concentration of the Si substrate [5,6], and the negative charges can still be observed when the Si substrate is covered by a thick SiO_2 layer [5]. Furthermore, the optical second harmonic generation measurements revealed that the positive charges at the Si/SiO_2 interface and positive bulk charges in the SiO_2 can be effectively compensated by the

* Corresponding author.
E-mail address: xiaohang.li@kaust.edu.sa (X. Li).

https://doi.org/10.1016/j.apsusc.2022.155099
Received 26 July 2022; Received in revised form 16 September 2022; Accepted 26 September 2022
Available online 5 October 2022

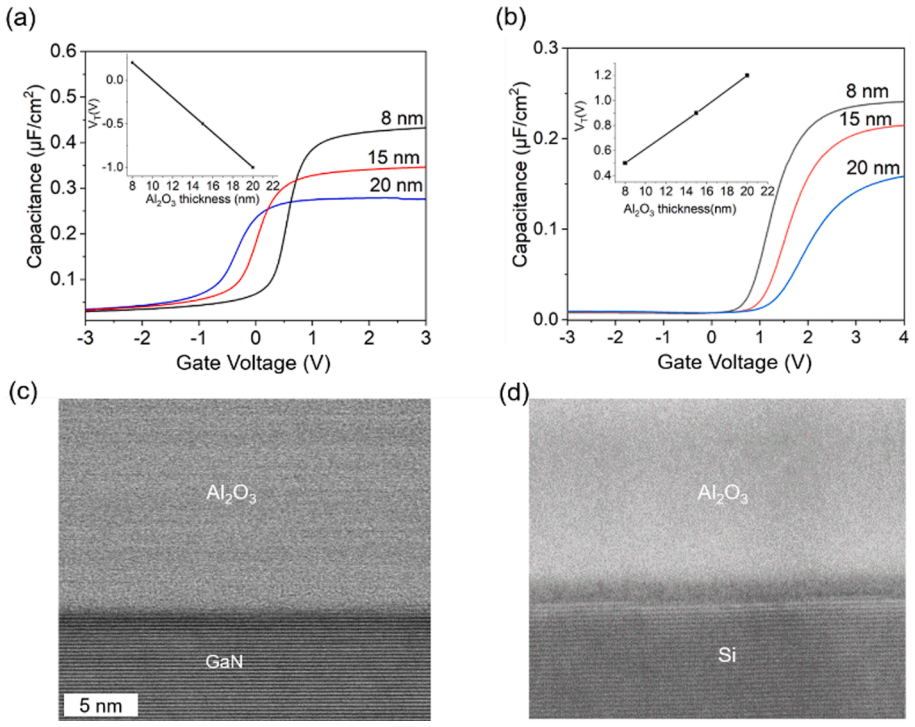

Fig. 1. C–V curves measured at 1 MHz with 8, 15, and 20 nm of Al_2O_3 on (a) GaN and (b) Si. Insets show the threshold voltage dependence on the thicknesses of Al_2O_3 on (a) GaN and (b) Si. TEM images of the (c) Al_2O_3/GaN and (d) Al_2O_3/Si H2s.

interfacial negative charges of Al_2O_3/Si H2 when Al_2O_3 the is deposited on the Si substrate [24,25].

Accurate positioning for the charges using typical electronic measurements such as capacitance-voltage (C–V) technique is difficult if the Al_2O_3/GaN or Al_2O_3/Si H2s are studied alone; therefore, many above-mentioned studies mistakenly attributed the origin of the charges of Al_2O_3/Si and Al_2O_3/GaN H2s to the defects inside Al_2O_3 itself, which is related to the intrinsic properties of Al_2O_3. However, the different polarity of charges at the Al_2O_3/GaN and Al_2O_3/Si H2s strongly suggests that the observed charges are not intrinsic to Al_2O_3; instead, they can be determined by the underlying semiconductor substrates on which Al_2O_3 is deposited.

2. Experiment section

Standard solvent cleaning was performed for n-type Si (1 0 0) samples and the GaN (0001) grown on c-plane sapphire substrates. The doping concentration of Si and GaN is 5.5×10^{15} cm^{-3} and 4.3×10^{16} cm^{-3}, respectively. Immediately after the cleaning process, the samples were transferred to an atomic layer deposition (ALD) chamber for the Al_2O_3 deposition after preheating for 5 min at 300 °C. One ALD cycle consisted of a 0.015 s TMA dose pulse and a 3 s O_2 plasma treatment with the power of 300 W, followed by a 3 s purge with N_2. The growth per cycle was 1.2 Å measured using ellipsometer (see Supporting Information Fig. S1). Different thicknesses (8, 15, and 20 nm) of Al_2O_3 were also deposited onto the GaN and Si samples under the same ALD conditions for the C–V measurements. The GaN and Si capacitors were prepared via the typical capacitor fabrication process, described in a previous literature [26]. A Keithley 4200A-SCS parameter analyzer was used for the C–V and I-V measurements of all the capacitors.

For X-ray photoelectron spectroscopy (XPS) measurements, after standard solvent cleaning process, Al_2O_3 scaled from the submonolayer to a few nanometers was deposited on both GaN and Si samples. Then, the samples were transferred to the XPS chamber immediately after the ALD process. The XPS signals of the C 1s, Al 2p, O1 s, Ga 3d, and Si 2p core levels were measured using an XPS AMICUS instrument. The XPS

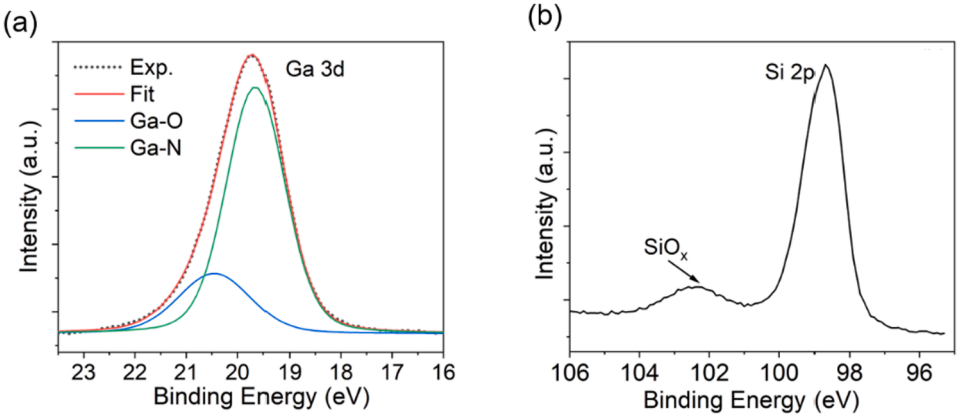

Fig. 2. XPS spectra of (a) Ga 3d of GaN and (b) Si 2p of Si.

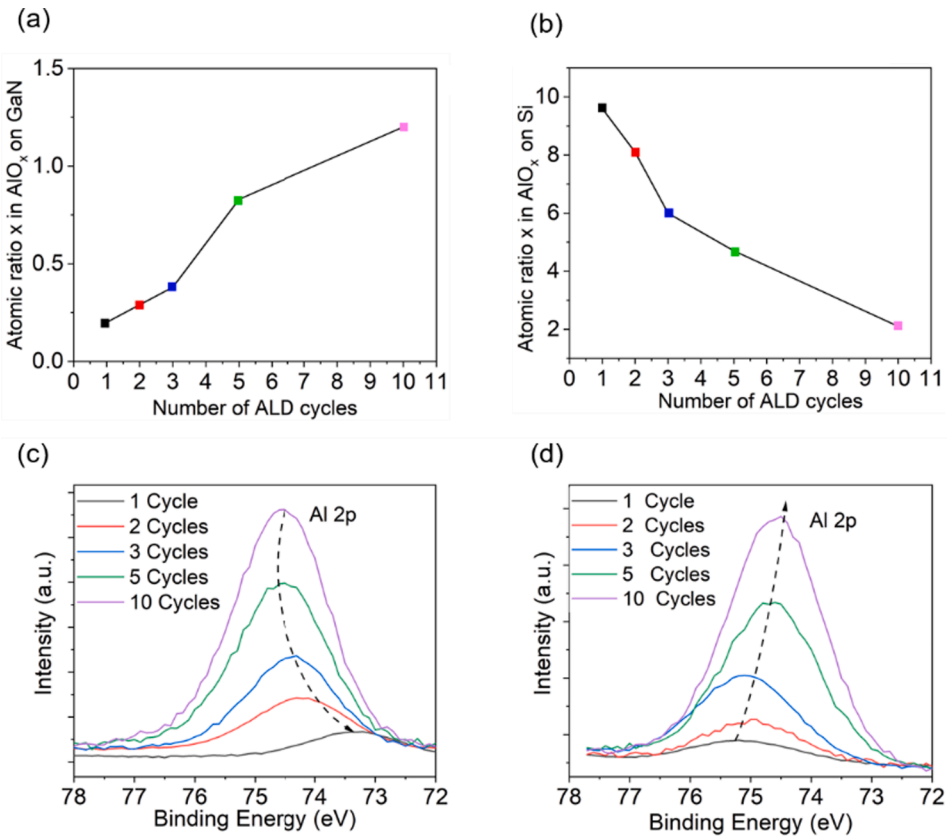

Fig. 3. O/Al ratios on (a) GaN and (b) Si coated with 1, 2, 3, 5, and 10 ALD cycles of Al_2O_3.. Binding energy positions of Al 2p with 1, 2, 3, 5, and 10 ALD cycles for Al_2O_3 on (c) GaN and (d) Si.

signals were calibrated with the C 1s binding energy of 284.8 eV. All XPS signals underwent Shirley background correction.

This study used DFT calculations to analyze the role of the Al and O interstitial defects at the interfaces of Al_2O_3/GaN and Al_2O_3/Si H2s. These calculations were performed using the Perdew–Burke–Ernzerhof version of the generalized gradient approximation for the exchange–correction potential, as was implemented in the plane–wave basis code of the Vienna ab initio simulation package. The cutoff energy was 450 eV, and a $6 \times 6 \times 1$ *k*-point gamma-centered mesh was used for the convergence test. Structural optimization was performed until the energy convergence criterion of 0.02 eV Å and the force of 10^{-5} eV were reached. The pseudopotential is described by the projector-augmented wave method to analyze the interactions between the ionic core and the valence electrons.

3. Results and discussion

C–V measurements were conducted on the Al_2O_3/GaN and Al_2O_3/Si capacitors [27]. The device structure for C–V measurements was shown in Fig. 2S. Fig. 1(a) and (b) show the C–V characteristics of the two systems with different Al_2O_3 thicknesses measured at 1 MHz. Under the positive gate bias, electrons transport from the semiconductor substrates to Al_2O_3, charge trapping and detrapping processes can lead to frequency dispersion in the accumulation region of the C–V curves (see Supporting Information Fig. S3(a) and (b)). The threshold voltage values can be estimated from the threshold dependence on the Al_2O_3 thickness [28] (see insets of Fig 0.1(a) and (b)). Depending on the Al_2O_3 thicknesses, different capacitance values were observed on the Al_2O_3/GaN and Al_2O_3/Si capacitors. Except from the insulator capacitance, interfacial traps, bulk states, and free carriers can also contribute to the total measured capacitance, leading to the derivation of the measured capacitance from proportional relationships with the Al_2O_3 thickness (Supporting Information Fig. S4). The gate leakage current can be suppressed to a lower value with the increased Al_2O_3 thickness (see Supporting Information Fig. S5(a) and (b)). When the Al_2O_3 thickness increased, the threshold voltage moved to a negative value in the Al_2O_3/GaN capacitor and to a positive value in the Al_2O_3/Si capacitor. The quantities of the interfacial charge densities can be deduced from the equation (2):

$$qV_{FB} = -qE_{ox}t_{ox} + (\varphi_b - \Delta E_c - \varphi_c \quad (2)$$

Here, V_{FB} is the flat-band voltage in the strongly accumulated capacitance; E_{ox} is the electrical field in the gate dielectric Al_2O_3; t_{ox} denotes the thickness of Al_2O_3; $\varphi_b$is the barrier height of Al_2O_3/Si and Al_2O_3/GaN; ΔE_c represents the conduction band offset at Al_2O_3/GaN and Al_2O_3/ Si interfaces; and φ_c is the energy separation between the conduction band and the Fermi level of GaN and Si [29]. The interfacial charge densities are calculated to be 5.3×10^{12} and -4.5×10^{12} cm^{-2} at the interfaces of Al_2O_3/GaN and Al_2O_3/Si H2s, respectively. The linearity of the threshold voltage versus the Al_2O_3 thickness plot shows the negligible influence of the bulk charges inside Al_2O_3 [28]. Fig. 1(c) and (d) show high-resolution transmission electron microscope (TEM) images of the Al_2O_3/GaN and Al_2O_3/Si H2s, respectively, the interfacial oxide layers were both observed at two interfaces.

XPS measurements were performed on the GaN and Si samples without any Al_2O_3 coating. Ga 3d spectrum was shown Fig. 2(a) and it was deconvolved into two components: Ga–N (at 19.6 eV) and Ga–O (at 20.4 eV). The presence of the Ga–O bonds in the Ga 3d spectrum indicates that a GaO_x layer was present; this layer is supposed to consist of ε- and γ-phases [30–33]. For the Si sample shown in Fig. 2(b), the Si 2p signal displays a clear double-peak spectra; the peak at 102.4 eV arises from the native SiO_x on the surface of the Si substrate [2–4]. After the XPS measurements, the samples were transferred into an ALD chamber to undergo 30 s O_2 plasma treatment at the power of 300 W at 300 °C.

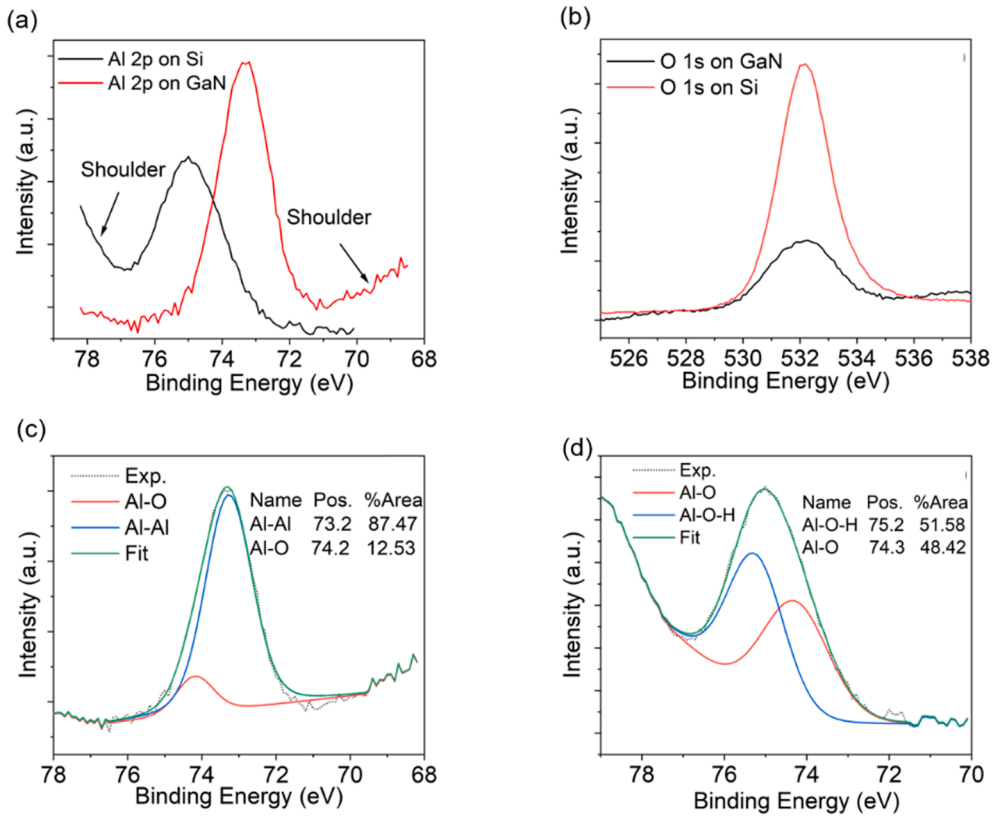

Fig. 4. (a) Al 2p spectra on the GaN and Si samples coated with one ALD cycle. (b) O 1s spectra on the Si and GaN samples without any Al_2O_3 coating. Deconvolution of the Al 2p spectra on the (c) GaN sample and (d) Si sample coated with one ALD cycle of Al_2O_3.

XPS measurements of the same samples were repeated. No obvious variations were observed in the Si 2p and Ga 3d XPS signals (see Supporting Information Fig. S6(a) and (b)), which implied that the native GaO_x and SiO_x layers under the ALD condition were thermally stable; this was consistent with previous reports [30].

XPS was then used to analyze the possible interactions between the surface layers of Si and GaN and Al_2O_3 in the monolayer regions to elucidate the origin of the positive and negative charges at the interfaces of the Al_2O_3/GaN and Al_2O_3/Si H2s, respectively. As illustrated in Fig. 3 (a) and (b), thickness-dependent Al_2O_3 scaled from the submonolayer to a few nanometers was deposited on both GaN and Si for XPS measurements. The O 1s contributions from the surface native oxides of GaN and Si were subtracted to obtain the O/Al atomic ratios of Al_2O_3 at the interfacial regions [2–4]. The O/Al ratios increased and decreased gradually to a stoichiometric value of 1.5 with increasing ALD cycles, yielding the ratios of 0.2 and 9.6 for one ALD cycle on GaN and Si, respectively.

The binding energies of Al 2p were then investigated to determine the origin of the nonstoichiometric O/Al atomic ratios at the interfaces of the two H2s and the results are shown in Fig. 3 (c) and (d). For the bulk Al_2O_3, the binding energy position of the Al 2p core–shell levels peaked at 74.3 eV, which was 1.2 eV higher than the binding energy position of the Al 2p when one ALD cycle of Al_2O_3 was coated onto GaN and 1 eV lower than the binding energy position of the Al 2p when one ALD cycle was coated onto Si. The dotted line in Fig. 3 (c) and (d) marked the peak position of Al 2p with different ALD cycles on GaN and Si. The binding energies of Al 2p core–shell levels on both the GaN and Si substrates shifted to 74.5 eV when 10 ALD cycles were coated onto the substrates. These values are very close to the binding energy position of the Al 2p core–shell levels in the bulk Al_2O_3 (74.3 eV) on both the GaN and Si substrates. This phenomenon is reasonable as XPS measurements are commonly used for the examination of material surfaces, it also indicates that non-idealities mainly locate at the interfaces of the two H2s.

The XPS signals of the Al 2p and O 1s core levels were further investigated to clarify the origin of the serious derivations of the O/Al atomic ratios from the stoichiometric values within the submonolayer region of Al_2O_3. After the GaN and Si samples were coated with one ALD cycle of Al_2O_3, the Al 2p XPS spectra were recorded and compared. Contrary to previous studies, no starting cycle was required for the absorption of the TMA molecules on the GaN and Si surfaces as the Al 2p signals were observed on both the surfaces with one ALD cycle as shown in Fig. 4(a) [4]. The binding energy positions of the Al 2p signals were different with a separation of 1.3 eV on the GaN and Si samples, indicating different bonding types of Al on the two sample surfaces. The integrated intensity of the Al 2p signals were 1.7 times higher on the GaN sample than on the Si sample, which implies that the sticking coefficient of the TMA molecules was higher for GaN than for Si at the time of molecules nucleation on the two sample surfaces during the first ALD cycle. In comparison with the Si surface, the existence of more TMA molecules on the GaN surface is favorable for the formation of Al–Al bonds. As shown in Fig. 4(a), shoulders are observed on the low binding energy side of GaN and on the high binding energy side of Si, which could be attributed to the background signals. To determine this results, the ALD and XPS processes were repeated using different samples. All the samples displayed evident shoulders with one ALD cycle, and these results excluded the possible fake XPS signals resulting from contaminations. The O 1s spectra from the surfaces of the GaN and Si samples without any Al_2O_3 coating are also presented in Fig. 4(b). The integrated intensity of the O 1s spectra is much higher on the Si surface than on the GaN surface which can be attributed to a thicker amorphous oxide layer on the Si surface as observed in Fig. 1 (c) and (d).

The Al 2p XPS spectra were deconvoluted into different bonding types to reveal the origin of the different binding energy positions of Al 2p on the surfaces of the GaN and Si. The Al 2p XPS spectra were both deconvoluted into two components for the GaN and Si samples covered with one ALD cycle: Al–Al (73.1 eV) and Al–O (74.2 eV) on the GaN

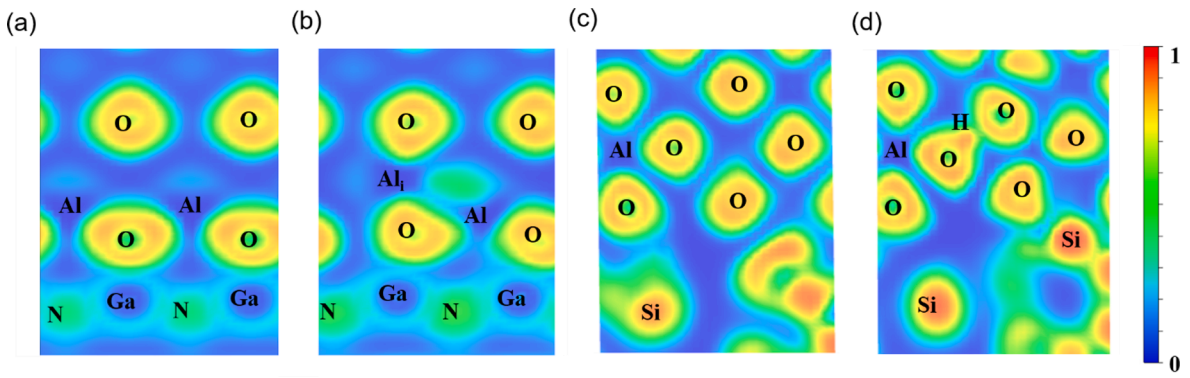

Fig. 5. 2D ELF images of the Al_2O_3/GaN H2 (a) without and (b) with the interstitial Al. 2D ELF images of the Al_2O_3/Si H2 (c) without and (d) with the interstitial OH group.

sample (see Fig. 4(c)) and Al–O–H (75.2 eV) and Al–O (74.3 eV) on the Si sample (see Fig. 4(d)); these findings are consistent with previous research results [34,35]. The integrated intensity of the Al–Al bonds account for nearly 88% of the entire Al 2p XPS spectral area on the GaN sample, and the Al–O–H bonds also account for 52% of the integrated intensity of the Al 2p XPS spectral area on the Si sample. A large number of Al–Al and Al–O–H bonds lead to excess Al and O atoms at the interfacial regions of Al_2O_3/GaN and Al_2O_3/Si H2s, respectively [35], which is consistent with the measured stoichiometry deviation of O/Al atomic ratios at the interfaces of the two H2s discussed above. Moreover, H cannot be detected via the XPS measurements, and the H atom that forms the Al–O–H bond comes most likely from the OH group absorbed on the Si surface [2].

Fig. 5(a)-(d) illustrate the two-dimensional (2D) electron localization function (ELF) images at the interfacial regions of the Al_2O_3/GaN and Al_2O_3/Si H2s without and with defects. The contours of the electron localization are labeled with the corresponding atoms in the images. The ELF value can vary from 0 to 1. A value less than 0.5 correspond to ionic bonds, while a value larger than 0.5 shows the formation of covalent bonds; an ELF value of 0.5 corresponds to the homogeneous electron gas, an indication of metal bonds [36]. As shown in Fig. 5(a)-(d), the electron localization of the O atoms is more distorted at the first Al–O layer of Al_2O_3 than in the bulk material, suggesting that more electron redistribution occurs at the interfacial region. One interstitial Al atom and one interstitial OH group are introduced into the interfacial regions of Al_2O_3/GaN and Al_2O_3/Si H2s in Fig. 5(b) and (d), respectively, in keeping with the results as measured using the XPS method. As shown in Fig. 5(b), the ELF value between the interstitial Al and the lattice Al is close to 0.5, indicating the formation of an Al–Al bond. The bond length between the interstitial Al and the lattice Al is 2.527 Å, which coincides well with the previous report on metallic Al–Al bonds [37]. Similar to the lattice Al, the interstitial Al can deplete charges, signifying the excess Al atom can lead to positive charges at the interfacial region of Al_2O_3/GaN H2. For the Al_2O_3/Si H2 with one interstitial OH group (see Fig. 5 (d)), the O atom forms bonds with H and Al, which verifies the formation of the Al–O–H bond as measured by the XPS method. A strong electron accumulation around the interstitial OH group confirms that the excess O can lead to negative charges at the interface of Al_2O_3/Si H2, as observed via C–V measurements.

4. Conclusion

Positive charges were observed at the interface of Al_2O_3/GaN H2, and the same level of negative charges were also observed at the interface of Al_2O_3/Si H2. The nonstoichiometric atomic ratios of O to Al from the bulk Al_2O_3 found at the interfaces of Al_2O_3/Si and Al_2O_3/GaN H2s were correlated with the interfacial charge polarity. Moreover, the nonstoichiometric cation/anion ratios of the interfacial dielectrics may not be an exclusive property of Al_2O_3 on the GaN and Si samples. For example, the charges observed at the interfaces of the following samples may also be attributed to the nonstoichiometric cation/anion ratios of the gate dielectrics near the interface regions: Al_2O_3/InGaAs, SiO_2/GaN, HfO_2/GaN, SiN/GaN and HfO_2/Si. The surface oxide layers of InGaAs, GaN and Si could also influence the initial growth of the Al_2O_3, SiO_2, HfO_2, and SiN thus to determine the interfacial cation/anion ratios of these dielectrics. XPS could also be a powerful tool to analyze the initial growth and interfacial atomic ratios of these dielectrics. This, however, requires further study.

CRediT authorship contribution statement

Chuanju Wang: Conceptualization, Methodology, Validation, Investigation, Writing – original draft, Writing – review & editing. **Feras AlQatari:** Methodology, Validation. **Vishal Khandelwal:** Methodology. **Rongyu Lin:** Investigation. **Xiaohang Li:** Resources, Project administration, Funding acquisition.

Declaration of Competing Interest

The authors declare the following financial interests/personal relationships which may be considered as potential competing interests: Chuanju wang reports was provided by KAUST. Chuanju wang reports a relationship with King Abdullah University of Science and Technology that includes: employment.

Data availability

Data will be made available on request.

Acknowledgment

The authors would like to acknowledge the support of KAUST Baseline BAS/1/1664-01-01, URF/1/3437-01-01, URF/1/3771-01-01, and URF/1/4374-01-01.

Data Availability

The data that support the findings of this study are available within the article.

Appendix A. Supplementary data

Supplementary data to this article can be found online at https://doi.org/10.1016/j.apsusc.2022.155099.

References

[1] D. Hiller, J. Göttlicher, R. Steininger, T. Huthwelker, J. Julin, F. Munnik, M. Wahl, W. Bock, B. Schoenaers, Structural Properties of Al–O Monolayers in SiO_2 on Silicon and the Maximization of Their Negative Fixed Charge Density, ACS Appl. Mater. Interfaces 10 (2018) 30495.

[2] V. Naumann, M. Otto, R.B. Wehrspohn, M. Werner, C. Hagendorf, Interface and material characterization of thin ALD-Al_2O_3 layers on crystalline silicon, Energy Procedia 27 (2012) 312–318.

[3] V. Naumann, M. Otto, R.B. Wehrspohn, C. Hagendorf, Chemical and structural study of electrically passivating Al_2O_3/Si interfaces prepared by atomic layer deposition, J. Vac. Sci. Technol., A 30 (4) (2012) 04D106.

[4] F. Werner, B. Veith, D. Zielke, L. Kühnemund, C. Tegenkamp, M. Seibt, R. Brendel, J. Schmidt, Electronic and chemical properties of the c-Si/Al_2O_3 interface, J. Appl. Phys. 109 (11) (2011) 113701.

[5] B. Hoex, J. Gielis, M. Van de Sanden, W. Kessels, On the c-Si surface passivation mechanism by the negative-charge-dielectric Al_2O_3, J. Appl. Phys. 104 (2008), 113703.

[6] B. Hoex, J. Schmidt, R. Bock, P.P. Altermatt, M.C.M. van de Sanden, W.M. M. Kessels, Excellent passivation of highly doped p-type Si surfaces by the negative-charge-dielectric Al_2O_3, Appl. Phys. Lett. 91 (11) (2007) 112107.

[7] D. Hiller, P.M. Jordan, K. Ding, M. Pomaska, T. Mikolajick, D. König, Deactivation of silicon surface states by Al-induced acceptor states from Al–O monolayers in SiO_2, J. Appl. Phys. 125 (1) (2019) 015301.

[8] D. Hiller, D. Tröger, M. Grube, D. König, T. Mikolajick, The negative fixed charge of atomic layer deposited aluminium oxide—a two-dimensional SiO_2/AlO_x interface effect, J. Phys. D Appl. Phys. 54 (27) (2021) 275304.

[9] K. Kim, J.H. Ryu, J. Kim, S.J. Cho, D. Liu, J. Park, I.-K. Lee, B. Moody, W. Zhou, J. Albrecht, Z. Ma, Band-bending of Ga-polar GaN interfaced with Al_2O_3 through ultraviolet/ozone treatment, ACS Appl. Mater. Interfaces 9 (20) (2017) 17576–17585.

[10] A. Hiraiwa, K. Horikawa, H. Kawarada, Space-charge-controlled field emission analysis of current conduction in amorphous and crystallized atomic-layer-deposited Al_2O_3 on GaN, J. Appl. Phys. 129 (19) (2021) 195303.

[11] L. Vauche, A. Chanuel, E. Martinez, M.-C. Roure, C. Le Royer, S. Bécu, R. Gwoziecki, M. Plissonnier, Study of an Al_2O_3/GaN Interface for Normally Off MOS-Channel High-Electron-Mobility Transistors Using XPS Characterization: The Impact of Wet Surface Treatment on Threshold Voltage V TH, ACS Appl. Electronic Mater. 3 (2021) 1170–1177.

[12] K. Aoshima, M. Horita, J. Suda, T. Hashizume, Impact of gamma-ray irradiation on capacitance–voltage characteristics of Al_2O_3/GaN MOS diodes with and without post-metallization annealing, Appl. Phys Express 14 (2021), 015501.

[13] Y. Ando, M. Deki, H. Watanabe, N. Taoka, A. Tanaka, S. Nitta, Y. Honda, H. Yamada, M. Shimizu, T. Nakamura, H. Amano, Impact of gate electrode formation process on Al_2O_3/GaN interface properties and channel mobility, Appl. Phys Express 14 (8) (2021) 081001.

[14] Y. Ando, K. Nagamatsu, M. Deki, N. Taoka, A. Tanaka, S. Nitta, Y. Honda, T. Nakamura, H.J.A.P.L. Amano, Low interface state densities at Al_2O_3/GaN interfaces formed on vicinal polar and non-polar surfaces, Appl. Phys. Lett. 117 (2020) 102102.

[15] M. Choi, J.L. Lyons, A. Janotti, C.G. Van de Walle, Impact of carbon and nitrogen impurities in high-κ dielectrics on metal-oxide-semiconductor devices, Appl. Phys. Lett. 102 (2013), 142902.

[16] X. Liu, C. Jackson, F. Wu, B. Mazumder, R. Yeluri, J. Kim, S. Keller, A. Arehart, S. Ringel, J. Speck, Electrical and structural characterizations of crystallized Al_2O_3/GaN interfaces formed by in situ metalorganic chemical vapor deposition, J. Appl. Phys. 119 (2016), 015303.

[17] M. Choi, A. Janotti, C.G. Van de Walle, Native point defects and dangling bonds in α-Al_2O_3, J. Appl. Phys. 113 (2013), 044501.

[18] J. Weber, A. Janotti, C. Van de Walle, Native defects in Al_2O_3 and their impact on III-V/Al_2O_3 metal-oxide-semiconductor-based devices, J. Appl. Phys. 109 (2011), 033715.

[19] T.-H. Hung, S. Krishnamoorthy, M. Esposto, D. Neelim Nath, P. Sung Park, S. Rajan, Interface charge engineering at atomic layer deposited dielectric/III-nitride interfaces, Appl. Phys. Lett. 102 (2013), 072105.

[20] K. Matsunaga, T. Tanaka, T. Yamamoto, Y. Ikuhara, First-principles calculations of intrinsic defects in Al_2O_3, Phys. Rev. B 68 (2003), 085110.

[21] B. Shin, J.R. Weber, R.D. Long, P.K. Hurley, C.G. Van de Walle, P.C. McIntyre, Origin and passivation of fixed charge in atomic layer deposited aluminum oxide gate insulators on chemically treated InGaAs substrates, Appl. Phys. Lett. 96 (15) (2010) 152908.

[22] K. Kimoto, Y. Matsui, T. Nabatame, T. Yasuda, T. Mizoguchi, I. Tanaka, A. Toriumi, Coordination and interface analysis of atomic-layer-deposition Al_2O_3 on Si (001) using energy-loss near-edge structures, Appl. Phys. Lett. 83 (21) (2003) 4306–4308.

[23] B. Hoex, M. Bosman, N. Nandakumar, W.M.M. Kessels, Silicon surface passivation by aluminium oxide studied with electron energy loss spectroscopy: Silicon surface passivation by aluminium oxide studied with electron energy loss spectroscopy, physica status solidi (RRL)–Rapid Research Letters 7 (11) (2013) 937–941.

[24] N.M. Terlinden, G. Dingemans, V. Vandalon, R.H.E.C. Bosch, W.M.M. Kessels, Influence of the SiO_2 interlayer thickness on the density and polarity of charges in Si/ SiO_2/Al_2O_3 stacks as studied by optical second-harmonic generation, J. Appl. Phys. 115 (3) (2014) 033708.

[25] G. Dingemans, N.M. Terlinden, M.A. Verheijen, M.C.M. van de Sanden, W.M. M. Kessels, Controlling the fixed charge and passivation properties of Si(100)/ Al_2O_3 interfaces using ultrathin SiO_2 interlayers synthesized by atomic layer deposition, J. Appl. Phys. 110 (9) (2011) 093715.

[26] C. Mizue, Y. Hori, M. Miczek, T. Hashizume, Capacitance–voltage characteristics of Al_2O_3 /AlGaN/GaN structures and state density distribution at Al_2O_3/AlGaN interface, Jpn. J. Appl. Phys. 50 (2011), 021001.

[27] R. Winter, I. Krylov, C. Cytermann, K. Tang, J. Ahn, P. McIntyre, M. Eizenberg, Fermi level pinning in metal/Al_2O_3/InGaAs gate stack after post metallization annealing, J. Appl. Phys. 118 (2015), 055302.

[28] M.A. Negara, M. Kitano, R.D. Long, P.C. McIntyre, Oxide Charge Engineering of Atomic Layer Deposited AlO_xN_y/Al_2O_3 Gate Dielectrics: A Path to Enhancement Mode GaN Devices, ACS Appl. Mater. Interfaces 8 (32) (2016) 21089–21094.

[29] S. Ganguly, J. Verma, G. Li, T. Zimmermann, H. Xing, D. Jena, Presence and origin of interface charges at atomic-layer deposited Al_2O_3/III-nitride heterojunctions, Appl. Phys. Lett. 99 (2011), 193504.

[30] K. Yuge, T. Nabatame, Y. Irokawa, A. Ohi, N. Ikeda, L. Sang, Y. Koide, T. Ohishi, Characteristics of Al_2O_3/native oxide/n-GaN capacitors by post-metallization annealing, Semicond. Sci. Technol. 34 (2019), 034001.

[31] Y. Irokawa, T.T. Suzuki, K. Yuge, A. Ohi, T. Nabatame, K. Kimoto, T. Ohnishi, K. Mitsuishi, Y. Koide, Low-energy ion scattering spectroscopy and reflection high-energy electron diffraction of native oxides on GaN (0001), Jpn. J. Appl. Phys. 56 (2017), 128004.

[32] K. Mitsuishi, K. Kimoto, Y. Irokawa, T. Suzuki, K. Yuge, T. Nabatame, S. Takashima, K. Ueno, M. Edo, K. Nakagawa, Electron microscopy studies of the intermediate layers at the SiO_2/GaN interface, Jpn. J. Appl. Phys. 56 (2017), 110312.

[33] Y. Irokawa, K. Mitsuishi, T.T. Suzuki, K. Yuge, A. Ohi, T. Nabatame, T. Ohnishi, K. Kimoto, Y. Koide, Electron microscopy and ultraviolet photoemission spectroscopy studies of native oxides on GaN (0001), Jpn. J. Appl. Phys. 57 (2018), 098003.

[34] M. Usman, M. Arshad, S.S. Suvanam, A. Hallén, Influence of annealing environment on the ALD-Al_2O_3/4H-SiC interface studied through XPS, J. Phys. D Appl. Phys. 51 (2018), 105111.

[35] I. Iatsunskyi, M. Kempiński, M. Jancelewicz, K. Załęski, S. Jurga, V. Smyntyna, Structural and XPS characterization of ALD Al_2O_3 coated porous silicon, Vacuum 113 (2015) 52–58.

[36] J. Jia, B. Li, S. Duan, Z. Cui, H. Gao, Monolayer MBenes: prediction of anode materials for high-performance lithium/sodium ion batteries, Nanoscale 11 (2019) 20307–20314.

[37] M.-C. Yang, M.-D. Su, Theoretical investigations of the reactivity of neutral molecules that feature an M [double bond, length as m-dash] M (M= B, Al, Ga, In, and Tl) double bond, New J. Chem. 43 (2019) 9364–9375.